JIPB Journal of Integrative Plant Biology

Two soybean bHLH factors regulate response to iron deficiency

Lin Li[1], Wenwen Gao[1], Qi Peng[1], Bin Zhou[2], Qihui Kong[1], Yinghui Ying[1] and Huixia Shou[1]*

1. State Key Laboratory of Plant Physiology and Biochemistry, College of Life Sciences, Zhejiang University, Hangzhou 310058, China
2. Institute of Crop Science, Anhui Academy of Agricultural Sciences, Hefei 230031, China
*Correspondence: Huixia Shou (huixia@zju.edu.cn)
doi: 10.1111/jipb.12651

Research Article

Abstract Iron is an indispensable micronutrient for plant growth and development. Limited bioavailability of Fe in the soil leads to iron deficiency chlorosis in plants and yield loss. In this study, two soybean basic helix-loop-helix transcription factors, GmbHLH57 and GmbHLH300, were identified in response to Fe-deficiency. Both transcription factors are expressed in roots and nodules, and are induced by Fe deficiency; these patterns were confirmed in transgenic hairy roots expressing constructs of the endogenous promoters fused to a GUS reporter gene. Bimolecular fluorescence complementation, yeast two-hybrid and coimmunoprecipitation (co-IP) assays indicated a physical interaction between GmbHLH57 and GmbHLH300. Studies on transgenic soybeans overexpressing *GmbHLH57* and *GmbHLH300* revealed that overexpression of each transcription factor, alone, results in no change of the responses to Fe deficiency, whereas overexpression of both transcription factors upregulated the downstream Fe uptake genes and increased the Fe content in these transgenic plants. Compared to wild type, these double overexpression transgenic plants were more tolerant to Fe deficiency. Taken together, our findings establish that GmbHLH57 and GmbHLH300 are important transcription factors involved in Fe homeostasis in soybean.

Edited by: Leon V. Kochian, University of Saskatchewan, Canada
Received Dec. 5, 2017; **Accepted** Mar. 21, 2018; **Online on** Mar. 23, 2018

INTRODUCTION

Iron (Fe) is an indispensable micronutrient for virtually all living organisms. In plants, it is required for a variety of biological processes, including photosynthesis, respiration and chlorophyll biosynthesis (Kobayashi and Nishizawa 2012; Briat et al. 2015). Although abundant Fe may exist in the earth's crust, Fe is poorly available for plants due to its limited solubility in neutral and alkaline soils, leading to Fe deficiency chlorosis (IDC) and yield losses in many crops (Guerinot and Yi 1994; Mori 1999). On the other hand, excess Fe may also cause damage to plant growth and development (Halliwell and Gutteridge 1992). Thus, Fe homeostasis in plants needs to be tightly maintained through sophisticated regulation networks.

To cope with Fe-deficiency challenge, plants have evolved two distinct strategies for Fe uptake from the soil (Römheld and Marschner 1986; Kobayashi and Nishizawa 2012). Non-graminaceous plants use Strategy I, in which protons and phenolic compounds are excreted to acidify the soil in order to increase the solubility of ferric iron (Fe^{3+}) (Santi and Schmidt 2009). Fe^{3+} is then reduced to ferrous iron (Fe^{2+}) by membrane-bound ferric-chelate reductase oxidase (FRO) (Robinson et al. 1999; Waters et al. 2002). Subsequently, Fe^{2+} is transported across the plasma membrane into root epidermis cells by the major Fe^{2+} transporter, IRT1 (Iron-regulated transporter) (Eide et al. 1996; Varotto et al. 2002; Vert et al. 2002). Graminaceous plants use Strategy II, a chelation strategy to acquire Fe. These plants respond to Fe shortage by releasing phytosiderophores that chelate with Fe^{3+} in the soil (Kobayashi et al. 2010). The Fe^{3+}-phytosiderophore complexes are transported into root cells, via transporters belonging to the yellow stripe (YS) or YS like (YSL) family of proteins (Curie et al. 2001).

A number of transcription factors (TFs) were shown to be involved in Fe uptake and homeostasis.

Tomato *FER* was the first characterized bHLH TF essential for the Fe-deficiency response (Ling et al. 2002). Fe-deficiency Induced Transcription Factor (FIT), the *Arabidopsis* ortholog of FER, plays a crucial role in the Fe-deficiency signaling pathway. FIT is involved in controlling both Fe deficiency responses at both the transcriptional and post-transcriptional level. Overexpressing *FIT*, alone, is not sufficient to activate Fe responses in *Arabidopsis* (Colangelo and Guerinot 2004; Jakoby et al. 2004; Yuan et al. 2005; Zhang et al. 2006). The expression of *AtFRO2* relies mainly on the transcription of *FIT*, while the expression of *AtIRT1* was not (Zhang et al. 2006). The interaction between FIT and AtbHLH38/39, two bHLH Ib subgroup family members, is required to activate the transcription of downstream genes, *AtIRT1* and *AtFRO2*, to enhance Fe uptake and tolerance to Fe-deficiency (Yuan et al. 2008).

In addition, plants overexpressing *AtbHLH39* and double-overexpressing *FIT*/*AtbHLH38* and *FIT*/*AtbHLH39* exhibited enhanced tolerance to cadmium (Cd) exposure, via increased Cd sequestration in roots and improved Fe homeostasis of shoots (Wu et al. 2012). Bimolecular fluorescence complementation (BiFC) and yeast two-hybrid assays demonstrated that AtbHLH100 and AtbHLH101, two additional bHLHs Ib subgroup members, interact with FIT. Plants overexpressing *FIT* together with *AtbHLH101* showed constitutive expression of *AtFRO2* and *AtIRT1* in roots (Wang et al. 2013). Offering a different opinion, another group suggested that AtbHLH100 and AtbHLH101 are more likely to regulate genes involved in the distribution of Fe within the plant, suggesting that they play a non-redundant role with AtbHLH38 and AtbHLH39 that have been reported to act in concert with FIT (Sivitz et al. 2012). While *FIT* is expressed solely in roots, the expression of *AtbHLH38/39/100/101* genes was induced by Fe deficiency in both roots and shoots (Wang et al. 2007). Similarly, the interaction between FER and SlbHLH068 is essential for the activation of *LeFRO1* and *LeIRT1* in tomato (Du et al. 2015). In other species, such as *Populus*, two bHLH genes (*PtFIT* and *PtIRO*) were isolated and characterized. *PtFIT* was only expressed in the root and elevated under Fe-deficiency, whereas *PtIRO* was rarely detected in all tested tissues (Huang and Dai 2015).

Fe-deficiency Induced Transcription Factor and AtbHLH38/39/100/101 participate in Fe homeostasis, as positive regulators, and POPEYE (PYE) functions as a negative regulator, to mediate Fe homeostasis, by interacting with IAA-Leucine Resistant 3 (ILR3), a bHLH IVc subgroup family member (Long et al. 2010). Recent studies have shown that AtbHLH34, AtbHLH104, ILR3 and AtbHLH115 function as homodimers or heterodimers to non-redundantly modulate Fe homeostasis by regulating the transcription of *AtbHLH38/39/100/101* (Zhang et al. 2015; Li et al. 2016; Liang et al. 2017).

Fe deficiency chlorosis is among the most common of nutrient stresses in soybean (*Glycine max* L.), especially when grown in calcareous soils (pH $>$ 8) (Froechlich and Fehr 1981). In addition to the general demand for Fe, as an essential micronutrient for plant growth, Fe is also important for symbiotic proteins, such as nitrogenase, leghemoglobin, ferredoxin and cytochrome in legumes (Appleby 1984; Tang et al. 1990; Ragland and Theil 1993; Dixon and Kahn 2004). A significant quantitative trait locus (QTL) was identified on soybean chromosome 3, explaining more than 70% of the phenotypic variation in IDC (Lin et al. 1997). This QTL was further associated with two adjacent candidate genes (Glyma03g28610/03g28630) encoding for bHLH TFs (Peiffer et al. 2012). As both genes are homologs of AtbHLH38, it was proposed that they may form heterodimers with the soybean FIT-like TF to function in Fe homeostasis (Peiffer et al. 2012). However, the soybean FIT-like protein, the formation of the putative heterodimer and their roles in Fe acquisition remain to be elucidated.

In this study, GmbHLH57 and GmbHLH300, the homologs of FIT and AtbHLH38/39/100/101, were isolated and characterized. Both transcripts were upregulated by Fe deficiency and solely expressed in soybean roots and nodules. GmbHLH57 or GmbHLH300 interact with each other. Characterization of transgenic soybean plants overexpressing either *GmbHLH57* or *GmbHLH300*, or both TF genes demonstrated that induction of the downstream Fe responses genes, *GmFRO2* and *GmIRT1*, requires both TFs. Our work offers an important foundation for studies on the Fe-deficient response in soybean.

RESULTS

Identification and analysis of *GmbHLH57* and *GmbHLH300* genes

To study the roles of the soybean bHLH TFs involved in Fe homeostasis, BLAST searches were performed

against the soybean genome database, using the amino acid sequences of FIT and AtbHLH38/39/100/101. A phylogenetic tree was constructed, based on the resulting list of bHLH TFs, to examine their evolutionary relationship between *Arabidopsis* and soybean (Figure S1A). Four putative proteins, named GmbHLH56 (Glyma.13G322100), GmbHLH57 (Glyma. 12G178500), GmbHLH58 (Glyma.12G081200) and GmbHLH59 (Glyma.11G192800), belonging to the IIIa subgroup of the bHLH proteins (Hudson and Hudson 2015), were identified as potential FIT orthologs. GmbHLH300 (Glyma.03G130600), along with GmbHLH320 (Glyma.03G130400), GmbHLH321 (Glyma.19G132500) and GmbHLH322 (Glyma.19G132600), are grouped together with AtbHLH38/39/100/101. Blastp results revealed that GmbHLH57 shared 62.3% peptide similarity with FIT, GmbHLH300 shared 63.9%, 58.1%, 63.1% and 39.2% similarity with AtbHLH38, AtbHLH39, AtbHLH100 and AtbHLH101, respectively (Figure S1B).

Amino acid sequence alignments indicated that both GmbHLH57 and GmbHLH300 contain a highly conserved bHLH motif (Figure S1C). Comparison of the coding and genomic DNA sequences established that *GmbHLH57* contains four exons and three introns in its genomic sequence, which is the same as that of the *FIT* gene (Figure S1D). GmbHLH300 contained three exons and two introns, which is more similar to AtbHLH101. Considering the high sequence similarity and possible functional redundancy between these bHLHs, GmbHLH57 and GmbHLH300 were selected as the candidates to further assess their role in the Fe deficiency response in soybean.

Expression profile of *GmbHLH57* and *GmbHLH300*

We next performed qRT-PCR assays to analyze the spatial expression pattern of *GmbHLH57* and *GmbHLH300* in various tissues; these assays established that *GmbHLH57* and *GmbHLH300* expression is confined to roots and nodules (Figure 1A). To examine expression of these TFs, in response to different nutrient deficiencies, we determined *GmbHLH57* and *GmbHLH300* transcript abundance in roots of soybean plants grown in N-, P-, K-, Fe-, Mn-, Cu- or Zn-deprived conditions. As shown in Figure 1B, *GmbHLH57* and *GmbHLH300* were markedly induced by Fe deficiency, whereas deficiency of other minerals had little effect on their expression.

A time-course experiment showed that *GmbHLH57* transcript was gradually elevated after Fe deficiency, with a maximum induction after 7 d (Figure 1C). After resupplying Fe to the nutrient solution, *GmbHLH57* expression subsequently decreased. Similarly, *GmbHLH300* was upregulated after 5 d, reaching a maximum after 7 d. Transcripts of *GmbHLH300* were dramatically reduced by the resupply of Fe, dropping to undetectable levels (Figure 1C).

To confirm the expression pattern of *GmbHLH57* and *GmbHLH300*, transgenic hairy roots expressing constructs of the *GmbHLH57* or *GmbHLH300* promoter driving the GUS reporter (P_{bHLH57}:GUS and $P_{bHLH300}$:GUS) were generated. Under Fe-sufficient condition, GUS staining of the P_{bHLH57}:GUS lines revealed that GmbHLH57 is expressed in the primary root, lateral roots and root nodules. Fe deficiency significantly increased GUS expression (Figure 2). A similar GUS staining pattern was observed in the $P_{bHLH300}$:GUS transgenic roots and nodules (Figure 2). These results were in agreement with our qRT-PCR results.

GmbHLH57 can interact with GmbHLH300 亚细胞定位

We next investigated the subcellular localization of GmbHLH57 and GmbHLH300 in tobacco cells using an agroinfiltration system. Here, GFP fluorescent signal was clearly localized to the cell nuclei (Figure S2), supporting the notion that GmbHLH57 and GmbHLH300 are putative TFs. Yeast two-hybrid 酵母双杂 assays were also conducted to investigate the interaction between GmbHLH57 and GmbHLH300. When the coding sequence of GmbHLH57 was fused with the DNA binding domain of GAL4, in the bait vector pGBKT7, it exhibited strong auto activation activity (Figure S3). In contrast, no auto-activation activity was observed in GmbHLH300 (Figure S3). Yeast cells carrying the plasmid pGADT7-GmbHLH57 with pGBKT7-GmbHLH300, grew well on the quadruple dropout agar plate (QDO, SD/-Leu/-Trp/-His/-Ade), similarly to the positive control (Figure 3A). These results showed that GmbHLH57 can interact with GmbHLH300, in yeast cells.

To confirm the protein interaction of GmbHLH57 and GmbHLH300 occurs, *in planta*, a BiFC assay was performed on tobacco leaves by Agrobacterium infiltration. When GmbHLH57 was fused to the C-terminal YFP fragment (GmbHLH57-cYFP) and GmbHLH300 fused to the N-terminal YFP fragment (GmbHLH300-nYFP), a strong fluorescent signal was detected in epidermal cell nuclei of tobacco leaves

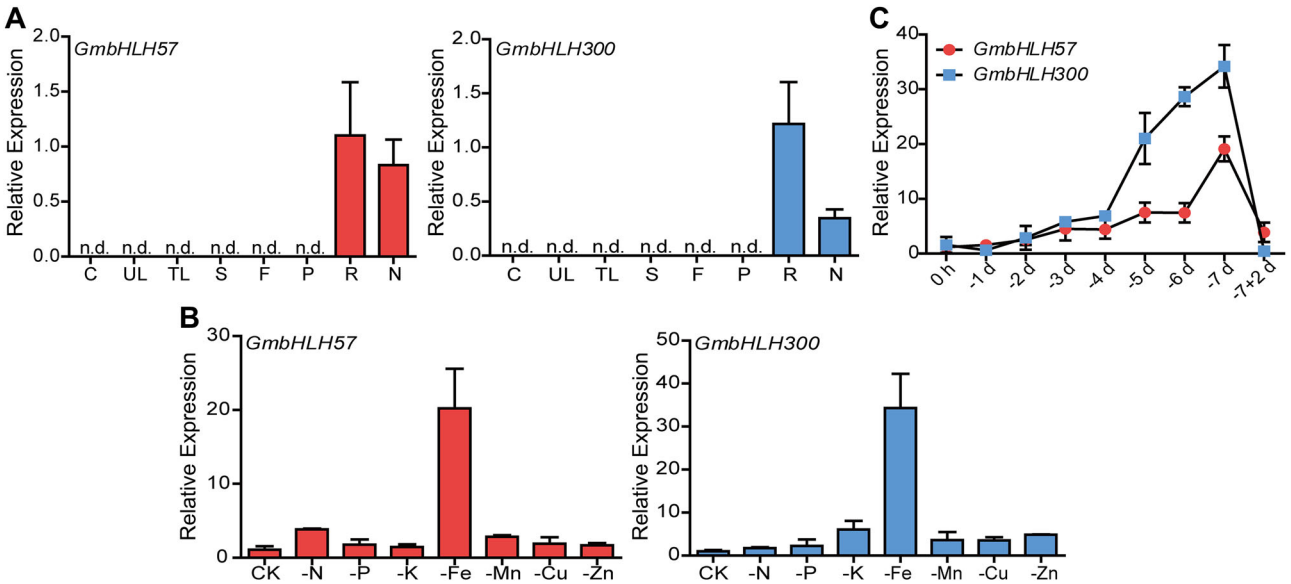

Figure 1. Expression profiling of *GmbHLH57* and *GmbHLH300* in wild-type (WT) soybean plants
(**A**) qRT-PCR analysis of *GmbHLH57* and *GmbHLH300* expression in different soybean tissues. Samples were collected from one-month-old soybean plants grown in modified Hoagland mineral nutrient solution. Cotyledon (C), unifoliate leaf (UL), trifoliolate leaf (TL), stem (S), flower (F), pod (P), root (R) and nodule (N). n.d., not detected. (**B**) Response of *GmbHLH57* and *GmbHLH300* in their roots to different nutrient stress. Ten-day-old seedlings were subjected to N, P, K, Fe, Mn, Cu and Zn deficiency for a week. (**C**) Time-course experiment of *GmbHLH57* and *GmbHLH300* response to Fe deficiency. Ten-day-old seedlings were transferred to nutrient solution without Fe supply. RNA was extracted from the roots at different times. Data are presented as mean $\pm$ *SD*, $n = 3$.

(Figure 3B). The negative control (nYFP and cYFP) failed to produce any YFP signal. In addition, GmbHLH57 displayed self-interaction, which was absent with GmbHLH300.

Co-immunoprecipitation studies were conducted using protein extracted from *N. benthamiana* leaves co-expressing 3Flag-GmbHLH57 (or 3Flag-GFP) and 4Myc-GmbHLH300. These assays indicated that 4Myc-GmbHLH300 was pulled down in the presence of 3Flag-GmbHLH57, but not in the presence of 3Flag-GFP (Figure 3C), indicating GmbHLH57 could interact with GmbHLH300. Taken together, these data support the hypothesis that GmbHLH57 interacts with GmbHLH300 to form a heterodimer in plant cells.

Enhanced tolerance to Fe deficiency is conferred by overexpressing both *GmbHLH57* and *GmbHLH300* in transgenic soybean

To explore the biological function of GmbHLH57 and GmbHLH300, transgenic lines overexpressing *GmbHLH57* (Ox57) or *GmbHLH300* (Ox300), driven by a modified CaMV 35S promoter, were generated using the soybean cotyledonary-node transformation system. Expression levels of *GmbHLH57* and *GmbHLH300* in these transgenic soybean lines were confirmed by qRT-PCR (Figure S4A). Among the confirmed transgenic lines, one line of each transgenic construct was selected for crossing studies. Considering the protein interaction of GmbHLH57 and GmbHLH300, double-overexpression lines (Ox57/300) were produced by crossing the single overexpression lines. Transgene transcript abundance for the particular transgenic event of Ox57 and Ox300 was measured by qRT-PCR. As expected, transcripts of *GmbHLH57* and *GmbHLH300* were significantly elevated in these overexpression lines (Figure S4B).

Under Fe-sufficient (+Fe) conditions, no differences in growth performance were detected between transgenic lines Ox57, Ox300 and WT plants. Double-overexpression line Ox57/300 displayed a decrease in shoot length and fresh weight (Figure 4A, B). After 3 d of −Fe treatment, Ox57, Ox300 and WT plants began to exhibit leaf chlorosis

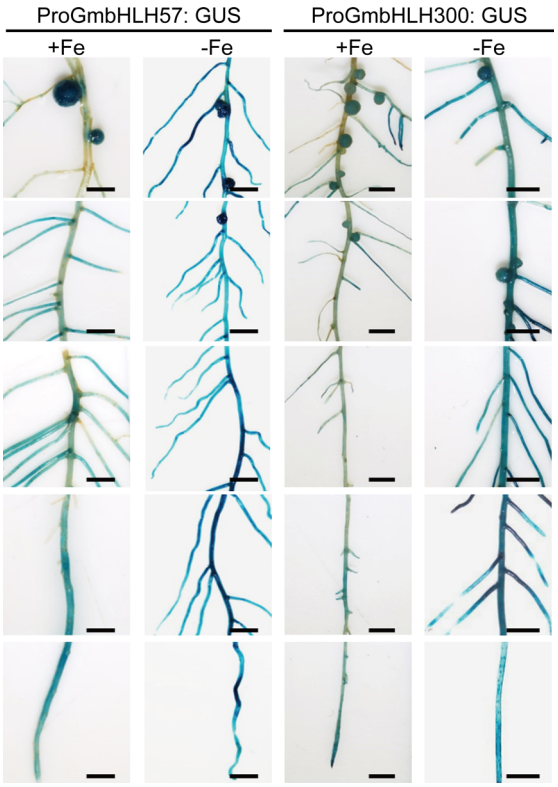

Figure 2. GUS staining in transgenic soybean hairy roots and nodules harboring promoter::GUS constructs
Soybean plants were grown in ± Fe nutrient solution for 7 d. Nodulated roots were excised and stained with GUS solution. Bars = 2 mm.

(data not shown), which became obvious after 7 d treatment (Figure 4A, B). In contrast, no leaf chlorosis was observed in Ox57/300 plants (Figure 4A, B). To assess the degree of leaf chlorosis caused by −Fe, the SPAD value of the 1st and 2nd trifoliate leaves was measured. Under Fe-sufficient conditions, the SPAD value of Ox57/300 was slightly higher than that of WT, Ox57 and Ox300. Under Fe-deficient conditions, the leaf SPAD values of the Ox57, Ox300, and Ox57/300 were significantly higher than that of WT. In addition, the leaf SPAD value of Ox57/300 was significantly higher than the single gene overexpression lines Ox57 and Ox300 (Figure 4C). The chlorophyll content in these plants was in accordance with the change of SPAD values (Figure 4D).

Fe concentrations in leaves, stems and roots of WT, Ox57, Ox300 and Ox57/300 plants were next measured by ICP-MS. Under both +Fe and −Fe conditions, no significant differences were observed among WT and the two single overexpression lines, whereas Ox57/300 contained significantly higher Fe than WT in leaves, stems, and roots (Figure 5).

Calcareous soil was used to further examine the Fe-deficient responses of Ox57, Ox300, Ox57/300 and wild-type (WT) plants. Three weeks after transplantation into calcareous soil, the newest leaves of Ox57, Ox300, and WT plants exhibited obvious Fe-deficient symptoms, whereas double-overexpression plants displayed remarkable tolerance to low Fe availability (Figure S5). These data support the hypothesis that overexpression of *GmbHLH57* and *GmbHLH300* enhances tolerance to Fe deficiency in soybean plants.

Overexpression of *GmbHLH57* and *GmbHLH300* activates the Fe deficiency response in soybean

Previous research demonstrated that *GmFRO2* and *GmIRT1*, orthologs of *AtFRO2* and *AtIRT1*, were induced in the near-isogenic line, Clark, under Fe stress. These two genes were considered to be downstream members of the Fe-deficiency signaling pathway (Peiffer et al. 2012). To investigate the effect of GmbHLH57 and GmbHLH300 on the expression of these Fe-responsive genes, qRT-PCR analysis was performed on *GmFRO2* and *GmIRT1* genes. Here, we established that *GmFRO2* and *GmIRT1* were indeed induced by Fe deficiency in roots of WT and Ox57, Ox300, and Ox57/Ox300 plants (Figure 6A). However, overexpression of either *GmbHLH57* or *GmbHLH300*, alone, did not affect the expression of *GmFRO2* and *GmIRT1*, but double overexpression of *GmbHLH57* and *GmbHLH300* significantly induced the expression of these Fe-deficiency-responsive genes. Fe-deficient treatment further increased the expression of *GmFRO2* and *GmIRT1* in Ox57/Ox300 plants (Figure 6A). Root Fe reductase activity was also analyzed to confirm the expression of *GmFRO2*. As shown in Figure 6B, Fe deficiency significantly induced the Fe reductase activities in WT and all transgenic soybean roots. Fe reductase activity of Ox57/300 was significantly higher than that of WT under both +Fe and −Fe conditions (Figure 6B).

Expression pattern analysis of soybean IVc bHLH subgroup members

Recent studies have shown that IVc subgroup bHLH TFs, AtbHLH34/104/105/115 activate the expression of PYE, FIT and AtbHLH38/39/100/101, under Fe-deficiency

conditions (Zhang et al. 2015; Li et al. 2016; Liang et al. 2017). To predict the upstream regulators of GmbHLH57 and GmbHLH300, we compared the soybean bHLHs with AtbHLHs. As shown in Figure 7, 10 IVc GmbHLH subgroup members, GmbHLH81-90, were classified with various similarities with the four AtbHLHs. It was reported that *AtbHLH34/104/105* are constantly expressed in both leaves and roots regardless of Fe supply (Liang et al. 2017). Whether the expression of *AtbHLH115* was affected by Fe supply remains controversial (Long et al. 2010; Liang et al. 2017).

To further investigate this matter, we performed qRT-PCR assays to determine the expression of the 10 soybean orthologs of *AtbHLH34/104/105* (Figure 7). Although expression of the *GmbHLH81-86* genes was not affected by Fe supply, those of *GmbHLH87-90* were upregulated by Fe deficiency in the roots (Figure 7). Diverse expression patterns of these soybean IVc

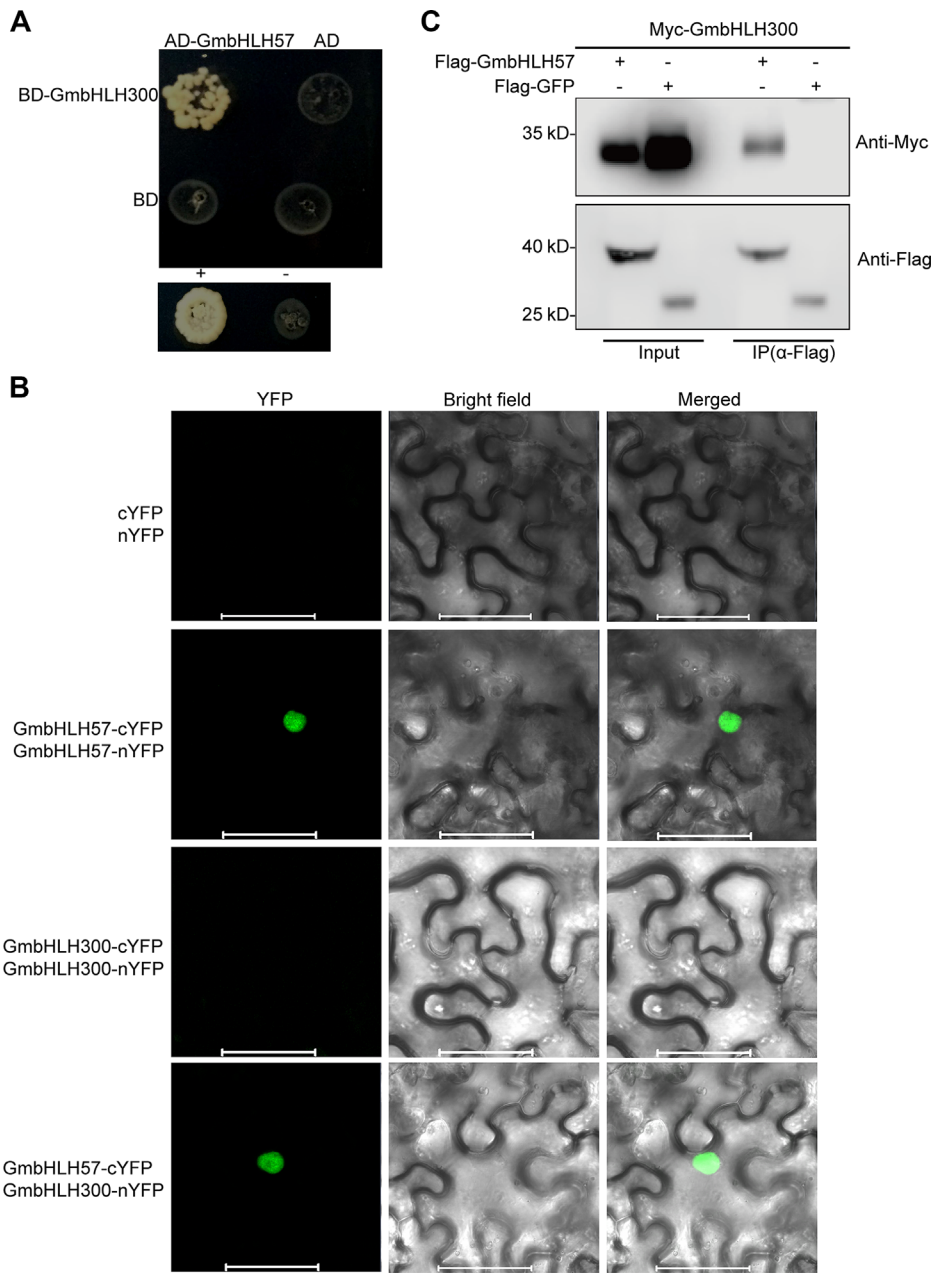

Figure 3. Continued.

bHLH subgroup members implied distinct roles in regulation of downstream genes. Given the important roles Fe plays in the growth of both soybean plants and symbiotic nitrogen-fixing root nodules, it is understandable that Fe homeostasis, in soybean, would be regulated more precisely than in *Arabidopsis*. Further studies to identify the direct upstream factor(s) of GmbHLH57 and GmbHLH300 would shed light on the fine-control mechanism of Fe homeostasis in soybean.

DISCUSSION

The bHLH proteins are a superfamily of TFs that participate in multiple biological processes (Massari and Murre 2000). Most members of this family have been characterized functionally in many plant species, with key roles being established in the regulation of plant development and stress responses. A total 319 bHLH-domain containing proteins was identified within the soybean genome (Hudson and Hudson 2015), with most having unknown functions. In the present study, eight soybean orthologs of AtbHLHs were identified, based on our BlastP results, and two, GmbHLH57 and GmbHLH300, identified as FIT and AtbHLH38/39 homologs were isolated and characterized.

Phylogenetic analysis revealed that GmbHLH57 and GmbHLH300 were clustered into two groups (Figure S1A). Amino acid sequence alignment showed that both have a conserved bHLH domain (Figure S1). The typical threonine-glutamate-arginine (T-E-R) motif was present in the GmbHLH57 basic region of the bHLH domain, at positions 7-11-12, which is in accordance with other members in the group, whereas the GmbHLH300 motif was histidine-glutamate-arginine (H-E-R) (Figure S1C). The T-E-R motif could bind to the G-box (5'-CACGTG-3') of promoters of downstream genes and the H-E-R motif could bind to the E-box (5'-CANNTG-3') region (Heim et al. 2003). These findings suggest that GmbHLH57 and GmbHLH300 may have different functions in soybean plants under stress conditions.

The interaction between GmbHLH57 and GmbHLH 300 was confirmed by BiFC, yeast two-hybrid and co-IP assays. GmbHLH57 also showed auto-activation activity in yeast cells, whereas GmbHLH300 did not (Figure S3). We thought the main reason for this difference was that GmbHLH300 could not correctly fold in yeast cells, thereby affecting protein activity. The transcriptional activation function of GmbHLH300, in soybean plants, needs to be confirmed by further studies. It has also been reported that orthologs of GmbHLH300 in *Arabidopsis*, AtbHLH38/39/100/101, showed no auto-activation activity in yeast cells (Yuan et al. 2008; Wang et al. 2013).

The roles of GmbHLH57 and GmbHLH300 in the Fe-deficiency response is similar to that in *Arabidopsis*, in which FIT needs to interact with AtbHLH38/39/100/101 to be functional. Although these two TFs are both induced by Fe deficiency, overexpression of each TF, alone, is insufficient to alter the expression of downstream target genes. This is likely because the function of some bHLH members relies on the formation of heterodimers with other bHLHs. In other words, both TFs are required for the activation of the downstream genes.

Figure 3. GmbHLH57 interacts with GmbHLH300

(**A**) Yeast two-hybrid assays establish an interaction between GmbHLH57 and GmbHLH300. Yeast transformants were cultured on selection medium DDO (double dropouts SD medium, −Leu/-Trp) and QDO (quadruple dropouts SD medium, −Leu/-Trp/-His/-Ade). Positive control (+), pGAD-SV40 mated with pGBK-53; negative control (−), pGAD-SV40 mated with pGBK-Lam. (**B**) Bimolecular fluorescence complementation showing an interaction between GmbHLH57 and GmbHLH300 in tobacco leaves. Coding sequences of GmbHLH57 and GmbHLH300 were fused to the vectors of nYFP and cYFP to generate transient expression plasmids GmbHLH57-nYFP, GmbHLH57-cYFP, GmbHLH300-nYFP, GmbHLH300-cYFP, respectively. Bars = 50 μm. (**C**) Co-IP assay of GmbHLH300 and GmbHLH57 in tobacco leaves. The 4Myc-GmbHLH300 and 3Flag-GmbHLH57 or 3Flag-GFP were co-expressed in tobacco leaves by agroinfiltration. Protein was immunoprecipitated with anti-FLAG M2 magnetic beads, and detected using Myc antibody.

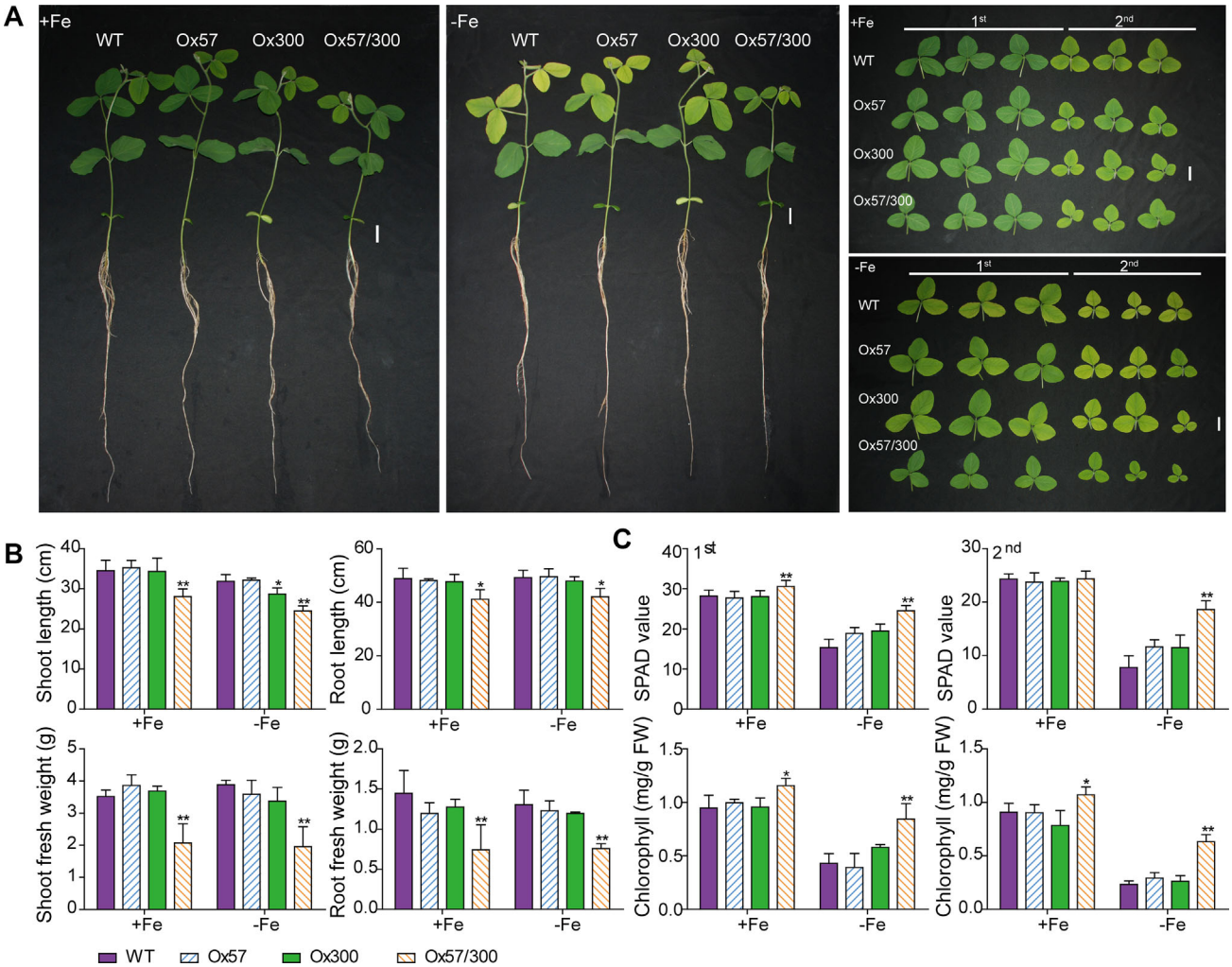

Figure 4. Characterization of WT and transgenic soybean plants that overexpress GmbHLH57 or/and GmbHLH300
(**A**) Growth performance of WT and overexpression plants under Fe-sufficient and −deficient conditions. Ten-day-old seedlings were grown on nutrient solution ± Fe for 7 d. First and second trifoliate leaves were detached phenotype analysis. (**B**) Plant length and biomass of WT and overexpression plants under ± Fe conditions. (**C**) SPAD value and total chlorophyll contents in WT and overexpression plants. Bar = 2 cm. Data are mean ± *SD*, $n = 3$. Significance of differences compared to WT is indicated by asterisks (LSD's ANOVA test; $^{*}P < 0.05$, $^{**}P < 0.01$).

AtbHLH38/39/100/101 were upregulated by Fe deficiency in both roots and leaves (Wang et al. 2007). Apart from regulating Fe uptake into the roots, they might also be involved in regulating Fe mobilization. The soybean orthologs of AtbHLH38/39/100/101, *GmbHLH300/320/321/322* are expressed in roots and nodules (Figure S6). Induction of expression for these soybean bHLH genes, under −Fe conditions, was only observed in roots (Figure S7). These findings suggest that regulation of these Ib subfamily bHLH genes differs between soybean and *Arabidopsis.*

Soybean differs from *Arabidopsis* in the production of a new plant organ, the root nodule, where Symbiotic Nitrogen Fixation (SNF) occurs. Due to the unique process of SNF, legumes have an increased demand for Fe (Tang et al. 1990). For instance, the important symbiotic protein, nitrogenase, requires Fe as a cofactor (Dixon and Kahn 2004). In addition, leghemoglobin, ferredoxin and cytochrome, essential constituents for symbiosis, possess a substantial amount of Fe (Appleby 1984; Ragland and Theil 1993; Dixon and Kahn 2004). In the current study, strong GUS expression was detected in nodules of the transgenic hairy roots when directed

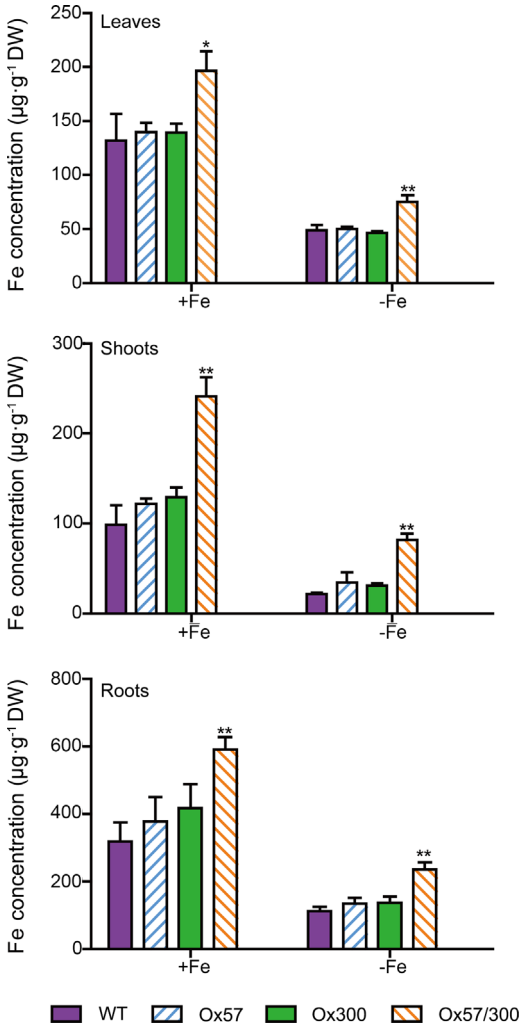

Figure 5. Fe concentrations in leaves, shoots and roots of WT and transgenic soybean plants overexpressing GmbHLH57 or/and GmbHLH300

Ten-day-old seedlings were transferred to nutrient solution containing 100 μM or 0 μM Fe (II)-EDTA and grown for 7 d. Fe concentrations in leaves, shoots and roots were measured by ICP-OES. Data are mean ± *SD*, $n = 3$. Significance ($P < 0.05$) of differences compared to WT is indicated by asterisks (LSD's ANOVA test; $^{*}P < 0.05$, $^{**}P < 0.01$).

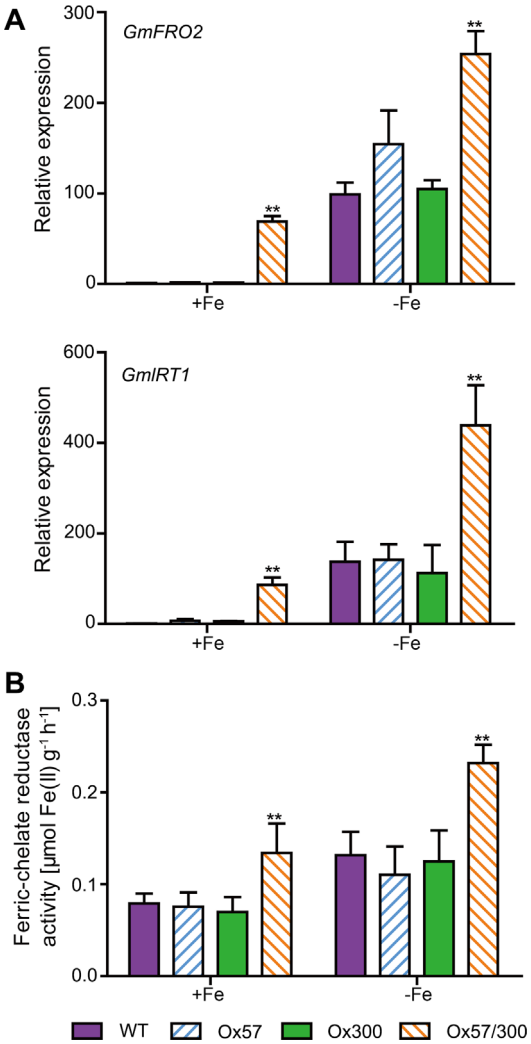

Figure 6. GmbHLH57 and GmbHLH300 activate expression of Fe deficiency-responsive genes

(**A**) Relative expression levels of *GmFRO2* and *GmIRT1* in roots of WT and GmbHLH57/300 overexpression plants. Ten-day-old seedlings were transferred to ± Fe nutrient solution for 7 d. (**B**) Ferric chelate reductase activity in WT and transgenic plants. Data are mean ± *SD*, $n = 3$. Significant differences from the corresponding wild type are indicated by asterisks (LSD's ANOVA test; $^{*}P < 0.05$, $^{**}P < 0.01$).

by the GmbHLH57 or GmbHLH300 promoter (Figure 2), suggesting that these TFs should have roles in soybean root nodule function.

Although double overexpression line Ox57/300 increased Fe concentration and nitrogenase activity of root nodules, in both Fe-sufficient or Fe-deficient conditions, compared to WT and the single Ox plants, it did not increase nodule number, size or fresh weight (Figure S8). This phenomenon can be attributed to the constitutive overexpression of GmbHLH57 or GmbHLH300 (Figure 4A). *GmbHLH57* and *GmbHLH300* are mainly expressed in the roots and nodules (Figure 1A). The 35S promoter-driven constitutive-overexpression increased their transcript abundance in all plant tissues, including shoots and leaves. We speculate that the increased expression of these two TFs, in shoots and leaves, may have resulted in an alteration

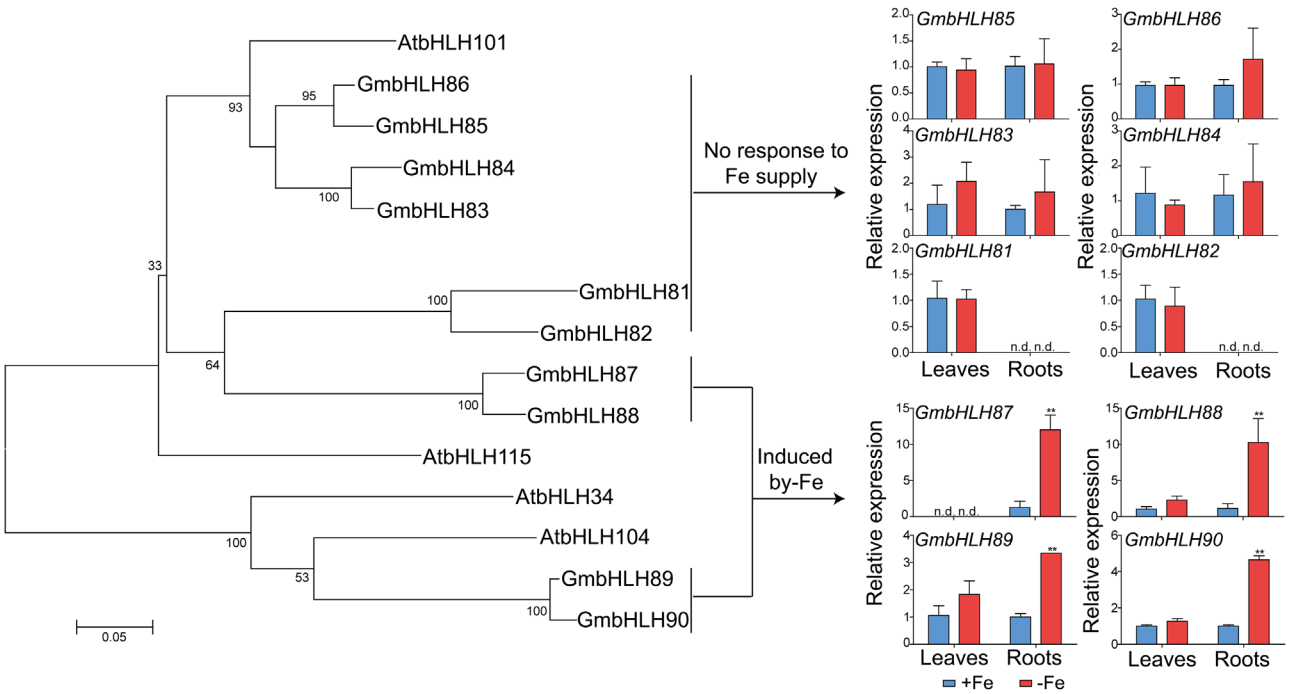

Figure 7. Phylogenetic and expression analysis of soybean homologs of AtbHLH IVc subgroup transcription factors

Phylogenetic tree was built based on amino acid sequences of AtbHLH IVc subgroup transcription factors and their soybean homologs using the Neighbor-Joining method in Mega version 6.0. *GmbHLH* transcripts were detected by qRT-PCR. Ten-day-old seedlings were transferred to nutrient solution ± Fe and grown for a week. RNA was extracted from leaves and roots. Data are mean ± *SD*, $n = 3$. n.d., not detected.

of Fe homeostasis and energy consumption, and consequently, caused a growth defect. Consistent with this notion, ectopic activity of genes in non-targeted tissues has been reported to be associated with the disruption of pattern formation and organogenesis, resulting in deleterious plant growth and development (Meijer and Murray 2001). Indeed, a similar phenotype was reported for AtbHLH34 or AtbHLH104 overexpression lines (Li et al. 2016). A further study with transgenic soybean plants overexpressing the TFs specifically in roots and nodules could unravel the roles played by these bHLH TFs in soybean nodules.

In conclusion, we have confirmed that a pair of bHLH TFs, GmbHLH57 and GmbHLH300, interact with each other to form heterodimers that likely control the Fe-deficient response in soybean. Both TFs were exclusively expressed in roots and nodules, and specifically induced by Fe deficiency. Using transgenic soybean approaches, we revealed that double overexpression of these TFs, in transgenic plants, enhanced tolerance to Fe deficiency and increased Fe content. Our findings identified the first components of the Fe-deficiency regulatory pathway in soybean.

MATERIALS AND METHODS

Plant materials and growth conditions

Soybean (*Glycine max cv.* Williams 82) was used in this study, and seeds were germinated in nursery pots with nutritional soil. After 4 d, seedlings were transferred to modified Hoagland mineral nutrient solution containing 7.5 mmol/L NH_4NO_3, 2.5 mmol/L $CaCl_2$, 1.5 mmol/L K_2SO_4, 1.0 mmol/L $MgSO_4 \cdot 7H_2O$, 0.38 μM $ZnSO_4 \cdot 7H_2O$, 1.57 μM $CuSO_4 \cdot 5H_2O$, 0.09 μM $(NH_4)_6Mo_7O_{24} \cdot 4H_2O$, 23.13 μM H_3BO_3, 4.57 μM $MnCl_2 \cdot 4H_2O$, 1.0 mmol/L $MnSO_4$, 0.25 mmol/L KH_2PO_4, 100 μM Fe(II)-EDTA, with pH 5.8. Fe deficiency (0 μM Fe) was initiated 6 d after transplanting. For the spatial expression pattern analysis, 4-day-old seedlings were inoculated with *Bradyrhizobium diazoefficiens* USDA110 for 1 h. Then seedlings were grown in a low-N nutrient solution (100 μM NH_4NO_3, the contents of other elements

remain unchanged). After 28 d, various tissues were collected for RNA extraction. For time-course analysis, plants were harvested on days 0, 1, 2, 3, 4, 5, 6 and 7 of Fe deficiency. On day 7 of Fe deficiency, Fe was re-supplied by adding 100 μM Fe(II)-EDTA, and plants were harvested 2 d later. For nutrient deficiency treatments, seedlings were transferred to nutrient solution deprived of nitrogen (-N), phosphate (-P), potassium (-K), -Fe, manganese (-Mn), zinc (-Zn) or copper (-Cu) for 7 d. For phenotypic analysis, 10-day-old seedlings were grown in nutrient solution with or without Fe(II)-EDTA for 7 d.

For soil experiments, 5-day-old seedlings were grown for 3 weeks on soil under normal and calcareous soil conditions. Calcareous soil was prepared by addition of 6% (w/w) calcium oxide to a final pH of 12.9. All experiments were carried out in a greenhouse with a day/night temperature of 28°C/24°C and a 12 h photoperiod (216 $\mu mol\ m^{-2}\ s^{-1}$). The nutrient solution was aerated continuously and changed every 3 d.

Yeast two-hybrid (Y2H) assays

Y2H assays were carried out, as previously described (Ying et al. 2017). The coding sequences of *GmbHLH57* and *GmbHLH300* were subcloned, in frame, into pGADT7-Rec and pGBKT7 to generate pGAD-Preys and pGBK-Baits, respectively. The pGBK-Baits constructs were transformed into yeast strain Y187 and pGAD-Preys into Y2Hgold (Clontech, CA, USA). Yeast was grown on-Leu/-Trp selection medium for the positive transformants and on-Leu/-Trp/-His/-Ade selection medium for the interaction studies. Primers used for vector construction are listed in Table S1.

Subcellular localization and BiFC

The coding sequences of *GmbHLH57* and *GmbHLH300*, without stop codes, were amplified and cloned into 35S-sGFP and BiFC vectors, using the GBclonart system. The following final vectors were obtained: GmbHLH57-sGFP, GmbHLH300-sGFP, GmbHLH57-nYFP, GmbHLH57-cYFP, GmbHLH300-nYFP, GmbHLH300-cYFP. Plasmids were transformed into *Agrobacterium tumefaciens* strain EHA105. *A. tumefaciens* cultures were infiltrated using a 1 mL syringe without a needle into the abaxial side of three-week-old *Nicotiana benthamiana* leaves. For the BiFC assay, equal volumes of an *A. tumefaciens* culture were mixed before infiltration into *N. benthamiana* leaves. After 48 to 72 h, fluorescent signals were detected using a Zeiss LSM710, confocal microscope system (Zeiss, Jena, Germany).

Co-immunoprecipitation assays

3Flag-GmbHLH57 (or 3Flag-GFP) and 4Myc-GmbHLH300 were transiently coexpressed in *N. benthamiana* leaves by *Agroinfiltration*. After 72 h of inoculation, infected leaves were harvested and used for protein extraction. After centrifugation, the cell lysate was incubated at 4°C with anti-FLAG M2 magnetic beads (Sigma-Aldrich, MO, USA) overnight. The FLAG fusion proteins were then eluted with 3X FLAG peptide and subject to immunoblot analysis.

Vector construction and soybean transformation

For overexpression constructs, the coding sequences of *GmbHLH57* (960 bp) and *GmbHLH300* (726 bp) were amplified and ligated into pMD-18Tvector (Takara, Dalian, China). After verification by DNA sequencing, these two fragments were cleaved by *Xba*I and cloned into binary vector pTF101.1-35s. Constructs were transformed into *Agrobacterium rhizogenes* strain LBA4404 by the heat shock method. The stable transformation was carried out via *Agrobacterium tumefaciens* mediated soybean cotyledon node transformation system as described previously (Song et al. 2013). Plants overexpressing *GmbHLH57* and *GmbHLH300* were named ox57 and ox300, respectively.

For expression pattern analysis, 2,195 bp upstream of the ATG start codon of *GmbHLH57* and 2,065 bp upstream of *GmbHLH300* were applied and cloned into pBI101.3 to generate P_{bHLH57}: GUS and $P_{bHLH300}$: GUS constructs. Constructs were transformed into *Agrobacterium rhizogenes* strain K599 and then transformed into soybean via hairy-root transformation (Kereszt et al. 2007).

To generate double overexpression transgenic plants, soybean sexual hybridization was performed between ox57 and ox300 transgenic lines planted during the 2014 summer season in the field at Hefei. The double overexpressing lines were named as ox57/300.

Histochemical GUS staining

The transgenic hairy roots under Fe-sufficient and −deficient nutrient solutions for 7 d. Roots were immersed immediately in GUS-staining buffer (100 mmol/L sodium phosphate, pH 7.0, 1 mmol/L 5-bromo-4-chloro-3-indolyl-b-D-glucuronidase), 1 mmol/L $K_4[Fe(CN)_6]$, 1 mmol/L $K_3[Fe(CN)_6]$, 0.5% TritonX-100and 20% methanol) at 37°C for 12 h. Afterwards,

samples were washed with 70% ethanol. Images were captured under a stereomicroscope.

Total chlorophyll content analysis

The SPAD value of the fully expanded leaves was measured by a portable chlorophyll meter (SPAD-502; Konica Minolta Sensing, JP). For total chlorophyll concentration, leaves were ground to powder in liquid nitrogen. 0.1 g powder was resuspended in 80% (v/v) acetone and stored at −20°C overnight. Then the mixture was centrifuged (4,000 g for 15 min at 4°C). The absorbance of the supernatant was read at 663 nm and 645 nm using a spectrophotometer.

Measurement of Fe concentration

Briefly, samples were dried for 3 d at 80°C and digested with 6 mL of 14 N HNO_3 and 1 mL of 8.8 M H_2O_2 at 150°C for 5 h. Fe concentration was measured using inductively coupled plasma mass spectrometry (ICP-MS, Agilent7500ce, CA, USA).

Ferric chelate reductase assays

Ferric chelate reductase assays were conducted, as described previously (Yi and Guerinot 1996). Briefly, soybean roots were submerged in 8 mL assay solution containing 0.2 mmol/L $CaSO_4 \cdot H_2O$, 0.1 mmol/L Fe(III)-EDTA, and 0.2 mmol/L BPDS. pH was adjusted to 5.5 with KOH. Assays were performed in darkness for 1 h. An identical assay solution containing no root was used as a blank. The pink-colored Fe(II)-BPDS complex was quantified at 553 nm.

Semi-quantitative RT-PCR and quantitative RT-PCR

Total RNA was extracted from different tissues of soybean plants using Trizol reagent according to manufacturer's instruction (Invitrogen, CA, USA). To eliminate DNA contamination, five micrograms of RNA were treated with RNase-free DNase I (Takara, Dalian, China). Reverse transcription was performed using the M-MLV reverse transcriptase (Promega, WI, USA). Semi-quantitative RT-PCR (semi-qRT-PCR) were carried out using gene-specific primers. *GmACTIN* was used as an internal control. qRT-PCR were conducted using LightCycler 480 SYBR Green I Master Kit on a LightCycler480machine (Roche Diagnostics, Manheim, Germany) according to the manufacturer's instructions. The soybean elongation factor EF-1a encoding gene, *GmTEFs1*, was used as the internal reference (Qin et al. 2012). The relative expression level was calculated using the formula $2^{-\triangle(\triangle cp)}$. For the quantification of each gene, at least three biological replicates were used. Primers for qRT-PCR analysis are given in Table S1.

Acetylene reduction assays

The acetylene reduction assay was used for measurement of nitrogenase activity (Hardy et al. 1968; Tejada-Jiménez et al. 2015). Nodules were quickly detached from soybean plants and placed in 100 mL rubber-capped penicillin bottles. 1 mL acetylene was injected into the bottles to replaced 1 mL air inside. Samples were incubated at 28°C for 1 h. Gas samples (1 mL) were analyzed by gas chromatography and mass spectrometry. The amount of ethylene produced was determined by measuring the height of the ethylene peak relative to background. Afterwards, nodule weights were determined.

ACKNOWLEDGEMENTS

This work was supported by the Ministry of Science and Technology of China (2016YFD0100703), the National Natural Science Foundation of China (31572189, 31771689), the Natural Science Foundation of Zhejiang Province (LZ16C 150001 and LY17C130002), and the Ministry of Education (B14027). We thank Professor Lei Zhang of the Anhui Academy of Agricultural Sciences for technical support.

AUTHOR CONTRIBUTIONS

H.S. and L.L. designed the experiments. Most of the experiments were performed by L.L. Other authors assisted in experiments and discussed the results. L.L. wrote the first draft of the manuscript. H.S. and other authors helped in revising the manuscript.

REFERENCES

Appleby CA (1984) Leghemoglobin and *Rhizobium* respiration. **Annu Rev Plant Physiol** 35: 443–478

Briat JF, Dubos C, Gaymard F (2015) Iron nutrition, biomass production, and plant product quality. **Trend Plant Sci** 20: 33–40

Colangelo EP, Guerinot ML (2004) The essential basic helix-loop-helix protein FIT1 is required for the iron deficiency response. **Plant Cell** 16: 3400–3412

Curie C, Panaviene Z, Loulergue C, Dellaporta SL, Briat JF, Walker EL (2001) Maize yellow stripe1 encodes a membrane protein directly involved in Fe(III) uptake. **Nature** 409: 346–349

Dixon R, Kahn D (2004) Genetic regulation of biological nitrogen fixation. **Nat Rev Micro** 2: 621–631

Du J, Huang Z, Wang B, Sun H, Chen C, Ling HQ, Wu H (2015) SlbHLH068 interacts with FER to regulate the iron-deficiency response in tomato. **Ann Bot** 116: 23–34

Eide D, Broderius M, Fett J, Guerinot ML (1996) A novel iron-regulated metal transporter from plants identified by functional expression in yeast. **Proc Natl Acad Sci USA** 93: 5624–5628

Froechlich DM, Fehr WR (1981) Agronomic performance of soybeans with differing levels of iron deficiency chlorosis on calcareous soil1. **Crop Sci** 21: 438–441

Guerinot ML, Yi Y (1994) Iron: Nutritious, noxious, and not readily available. **Plant Physiol** 104: 815–820

Halliwell B, Gutteridge JMC (1992) Biologically relevant metal ion-dependent hydroxyl radical generation An update. **FEBS Lett** 307: 108–112

Hardy RWF, Holsten RD, Jackson EK, Burns RC (1968) The acetylene-ethylene assay for N2 fixation: Laboratory and field evaluation. **Plant Physiol** 43: 1185–1207

Heim MA, Jakoby M, Werber M, Martin C, Weisshaar B, Bailey PC (2003) The basic helix–loop–helix transcription factor family in plants: A genome-wide study of protein structure and functional diversity. **Mol Biol Evol** 20: 735–747

Huang D, Dai W (2015) Molecular characterization of the basic helix-loop-helix (*bHLH*) genes that are differentially expressed and induced by iron deficiency in *Populus*. **Plant Cell Rep** 34: 1211–1224

Hudson KA, Hudson ME (2015) A classification of basic helix-loop-helix transcription factors of soybean. **Int J Genomics** 2015: 1–10

Jakoby M, Wang HY, Reidt W, Weisshaar B, Bauer P (2004) FRU (BHLH029) is required for induction of iron mobilization genes in *Arabidopsis thaliana*. **FEBS Lett** 577: 528–534

Kereszt A, Li D, Indrasumunar A, Nguyen CDT, Nontachaiyapoom S, Kinkema M, Gresshoff PM (2007) Agrobacterium rhizogenes-mediated transformation of soybean to study root biology. **Nat Protocols** 2: 948–952

Kobayashi T, Nakanishi H, Nishizawa NK (2010) Recent insights into iron homeostasis and their application in graminaceous crops. **Proc Jpn Acad Ser B** 86: 900–913

Kobayashi T, Nishizawa NK (2012) Iron uptake, translocation, and regulation in higher plants. **Annu Rev Plant Biol** 63: 131–152

Li X, Zhang H, Ai Q, Liang G, Yu D (2016) Two bHLH transcription factors, bHLH34 and bHLH104, regulate iron homeostasis in *Arabidopsis thaliana*. **Plant Physiol** 170: 2478–2493

Liang G, Zhang H, Li X, Ai Q, Yu D (2017) bHLH transcription factor bHLH115 regulates iron homeostasis in *Arabidopsis thaliana*. **J Exp Bot** 68: 1743–1755

Lin S, Cianzio S, Shoemaker R (1997) Mapping genetic loci for iron deficiency chlorosis in soybean. **Mol Breed** 3: 219–229

Ling HQ, Bauer P, Bereczky Z, Keller B, Ganal M (2002) The tomato fer gene encoding a bHLH protein controls iron-uptake responses in roots. **Proc Natl Acad Sci USA** 99: 13938–13943

Long TA, Tsukagoshi H, Busch W, Lahner B, Salt DE, Benfey PN (2010) The bHLH transcription factor POPEYE regulates response to iron deficiency in *Arabidopsis* roots. **Plant Cell** 22: 2219–2236

Massari ME, Murre C (2000) Helix-loop-helix proteins: Regulators of transcription in eucaryotic organisms. **Mol Cell Biol** 20: 429–440

Meijer M, Murray JAH (2001) Cell cycle controls and the development of plant form. **Curr Opin Plant Biol** 4: 44–49

Mori S (1999) Iron acquisition by plants. **Curr Opin Plant Biol** 2: 250–253

Peiffer GA, King KE, Severin AJ, May GD, Cianzio SR, Lin SF, Lauter NC, Shoemaker RC (2012) Identification of candidate genes underlying an iron efficiency quantitative trait locus in soybean. **Plant Physiol** 158: 1745–1754

Qin L, Zhao J, Tian J, Chen L, Sun Z, Guo Y, Lu X, Gu M, Xu G, Liao H (2012) The high-affinity phosphate transporter GmPT5 regulates phosphate transport to nodules and nodulation in soybean. **Plant Physiol** 159: 1634–1643

Römheld V, Marschner H (1986) Evidence for a specific uptake system for iron phytosiderophores in roots of grasses. **Plant Physiol** 80: 175–180

Ragland M, Theil EC (1993) Ferritin (mRNA, protein) and iron concentrations during soybean nodule development. **Plant Mol Biol** 21: 555–560

Robinson NJ, Procter CM, Connolly EL, Guerinot ML (1999) A ferric-chelate reductase for iron uptake from soils. **Nature** 397: 694–697

Santi S, Schmidt W (2009) Dissecting iron deficiency-induced proton extrusion in *Arabidopsis* roots. **New Phytol** 183: 1072–1084

Sivitz AB, Hermand V, Curie C, Vert G (2012) *Arabidopsis* bHLH100 and bHLH101 control iron homeostasis via a FIT-independent pathway. **PLoS ONE** 7: e44843

Song ZY, Tian JL, Fu WZ, Li L, Lu LH, Zhou L, Shan ZH, Tang GX, Shou HX (2013) Screening Chinese soybean genotypes for Agrobacterium-mediated genetic transformation suitability. **J Zhejiang Univ-SC B** 14: 289–298

Tang C, Robson AD, Dilworth MJ (1990) The role of iron in nodulation and nitrogen fixation in *Lupinus angustifolius* L. **New Phytol** 114: 173–182

Tejada-Jiménez M, Castro-Rodríguez R, Kryvoruchko I, Lucas MM, Udvardi M, Imperial J, González-Guerrero M (2015) Medicago truncatula natural resistance-associated macrophage protein1 is required for iron uptake by rhizobia-infected nodule cells. **Plant Physiol** 168: 258–272

Varotto C, Maiwald D, Pesaresi P, Jahns P, Salamini F, Leister D (2002) The metal ion transporter IRT1 is necessary for iron

homeostasis and efficient photosynthesis in *Arabidopsis thaliana*. **Plant J** 31: 589–599

Vert G, Grotz N, Dédaldéchamp F, Gaymard F, Guerinot ML, Briat JF, Curie C (2002) IRT1, an *Arabidopsis* transporter essential for iron uptake from the soil and for plant growth. **Plant Cell** 14: 1223–1233

Wang HY, Klatte M, Jakoby M, Bäumlein H, Weisshaar B, Bauer P (2007) Iron deficiency-mediated stress regulation of four subgroup Ib BHLH genes in *Arabidopsis thaliana*. **Planta** 226: 897–908

Wang N, Cui Y, Liu Y, Fan H, Du J, Huang Z, Yuan Y, Wu H, Ling H-Q (2013) Requirement and functional redundancy of Ib subgroup bHLH proteins for iron deficiency responses and uptake in *Arabidopsis thaliana*. **Mol Plant** 6: 503–513

Waters BM, Blevins DG, Eide DJ (2002) Characterization of FRO1, a pea ferric-chelate reductase involved in root iron acquisition. **Plant Physiol** 129: 85–94

Wu H, Chen C, Du J, Liu H, Cui Y, Zhang Y, He Y, Wang Y, Chu C, Feng Z, Li J, Ling HQ (2012) Co-overexpression FIT with AtbHLH38 or AtbHLH39 in *Arabidopsis*-enhanced cadmium tolerance via increased cadmium sequestration in roots and improved iron homeostasis of shoots. **Plant Physiol** 158: 790–800

Yi Y, Guerinot ML (1996) Genetic evidence that induction of root Fe(III) chelate reductase activity is necessary for iron uptake under iron deficiency. **Plant J** 10: 835–844

Ying Y, Yue W, Wang S, Li S, Wang M, Zhao Y, Wang C, Mao C, Whelan J, Shou H (2017) Two h-type thioredoxins interact with the E2 ubiquitin conjugase PHO2 to fine-tune phosphate homeostasis in rice. **Plant Physiol** 173: 812–824

Yuan Y, Wu H, Wang N, Li J, Zhao W, Du J, Wang D, Ling HQ (2008) FIT interacts with AtbHLH38 and AtbHLH39 in regulating iron uptake gene expression for iron homeostasis in *Arabidopsis*. **Cell Res** 18: 385–397

Yuan YX, Zhang J, Wang DW, Ling HQ (2005) AtbHLH29 of *Arabidopsis thaliana* is a functional ortholog of tomato FER involved in controlling iron acquisition in strategy I plants. **Cell Res** 15: 613–621

Zhang J, Liu B, Li M, Feng D, Jin H, Wang P, Liu J, Xiong F, Wang J, Wang HB (2015) The bHLH transcription factor bHLH104 interacts with IAA-LEUCINE RESISTANT3 and modulates iron homeostasis in *Arabidopsis*. **Plant Cell** 27: 787–805

Zhang J, Zhu HF, Liang H, Liu KF, Zhang AM, Ling HQ, Wang DW (2006) Further analysis of the function of AtBHLH29 in regulating the iron uptake process in *Arabidopsis thaliana*. **J Integr Plant Biol** 48: 75–84

SUPPORTING INFORMATION

Additional Supporting Information may be found online in the supporting information tab for this article: http://onlinelibrary.wiley.com/doi/10.1111/jipb.12651/suppinfo

Figure S1. Phylogenetic analysis and alignments of bHLHs involved in Fe homeostasis

(**A**) Phylogenetic tree of FIT, bHLH38/39/100/101, FER and their homologs in soybean. Amino acid sequences were used and the evolutionary assessment was conducted in MEGA6, via the neighbor-joining method. (**B**) Similarity matrix for FIT, AtbHLH38/39/100/101 and their homologs in soybean. (**C**) Amino acids sequence alignment of FER, FIT, AtbHLH38/39/100/101 and their homologs in soybean. The bHLH domains are highlighted by red boxes. (**D**) Gene structure comparison between GmbHLH57, GmbHLH300 and *Arabidopsis* homologs. 5'-UTR and 3'-UTR (white boxes), CDS (black boxes), introns are indicated by thin lines.

Figure S2. Subcellular localization of GmbHLH57 and GmbHLH300 in tobacco leaves

Fluorescent signal was detected with a confocal laser scanning microscope. Bars = 50 μm.

Figure S3. Validation of auto-activation activities of bait vectors in yeast two-hybrid assays

Coding sequences of GmbHLH57 and GmbHLH300 were cloned, in frame, into pGBKT7 bait vectors. Yeast strain Y2HGold cells were transformed with these bait constructs and grown on SD/-W (lacking Trp) plates. Auto-activation activities were assessed by the growth of yeast colonies on SD/-WHA (lacking Trp, His, and Ade) plates for 3 d.

Figure S4. Identification of *GmbHLH57* and *GmbHLH300* overexpression lines

(**A**) Reverse transcript PCR analysis of overexpression transgenic lines. Expression of *GmACTIN* was used as the internal control. (**B**) qRT-PCR analysis of one representative overexpression transgenic of Ox57, Ox300 and Ox57/300. RNA was extracted from leaves of fourteen-day-old seedlings. Expression of *GmTefs1* was used as the control. All data are mean ± *SD*, $n = 3$.

Figure S5. Phenotypes of WT and *GmbHLH57* and *GmbHLH300* overexpression soybean plants grown in alkaline soil

Seeds were germinated on normal soil for 5 d, then transferred to soil containing 6% calcium oxide for three weeks.

Figure S6. Expression analysis of *GmbHLH300/320/321/322* in different tissues of soybean plants

Data are from Phytozome (https://phytozome.jgi.doe.gov/pz/portal.html). n.d., not detected.

Figure S7. Expression analysis of *GmbHLH300/320/321/322* in response to different Fe supply conditions
Ten-day-old seedlings were transferred to nutrient solution ± Fe and grown for 7 d. RNA was extracted from leaves and roots. All data are mean ± *SD*, $n = 3$. n.d., not detected. Significant differences are indicated by asterisks (LSD's ANOVA test; $^{*}P < 0.05$, $^{**}P < 0.01$).

Figure S8. Effect of Fe deficiency on nodulation in WT and overexpression plants
Nodule number (**A**), nodule fresh weight (**B**), nodule size (**C**), acetylene reduction activity (ARA) of nitrogenase (**D**), Fe concentration in the nodules (**E**). Four-day-old seedlings inoculated with rhizobia were grown in +Fe nutrient solution for 17 d, then transferred to–Fe solution and grown for two weeks. Data are mean ± *SD*, $n = 3$. Significance ($P < 0.05$) of differences compared to WT is indicated by asterisks (LSD's ANOVA test; $^{*}P < 0.05$, $^{**}P < 0.01$).

Table S1. Primers used in this work

Scan using WeChat with your smartphone to view JIPB online

Scan with iPhone or iPad to view JIPB online